Struct Chem (2014) 25:1837–1846
DOI 10.1007/s11224-014-0459-6

ORIGINAL RESEARCH

Arene-fused 1,2-oxazole N-oxides and derivatives. The impact of the N–O dipole and substitution on their aromatic character and reactivity profile. Can it be a useful structure in synthesis? A theoretical insight

Paweł Kozielewicz · Demeter Tzeli · Petros G. Tsoungas · Mire Zloh

Received: 6 May 2014 / Accepted: 1 June 2014 / Published online: 27 June 2014

Abstract DFT calculations have shown that the N–O dipole of benzene- and naphthalene-fused 1,2-oxazole N-oxides causes a distortion of their σ and π frame, concentrated on the 1,2-oxazole ring, such that it increases its susceptibility to opening. The distortion forces the benzene ring into some diene geometry, thus, reducing π delocalization over the bi- or tricyclic structure and ultimately their aromatic character. C-3 substitution has a marked influence mainly on the naphthalene-fused N-oxides. C-5 and particularly C-6 substitution, as the position of most extended interaction with the N–O dipole through the π ring density, contribute to the distortion of the 1,2-oxazole geometry and thereby to the decrease of aromaticity of the structure. Bond uniformity (I_A), average bond order (ABO) and Harmonic Oscillator Model of Aromaticity (HOMA) indices have been recruited to measure aromaticity changes. I_A and ABO appear to be more credible to 1,2-benzoxazole N-oxides and 1,2-naphthoxazole N-oxides, respectively, while HOMA has been found equally reliable to both. Hardness and dipole moments follow similar trends. Energies, localization and separation of the four frontiers orbitals, i.e. HO, HO−1, and LU, LU+1, indicate a rather notable aromatic character of the N-oxides. Their reactivity profile, portrayed by descriptors such as Fukui and electro(nucleo)philicity Parr functions, shows good agreement with experimental outcomes towards electrophiles but succumbs to discrepancies towards nucleophiles due to the susceptibility of the hetero-ring to opening. The "push–pull" character of the N–O dipole and more importantly the extent of its double bonding direct site selectivity.

Keywords Benzo-fused 1,2-oxazole N-oxide · Naphtho-fused 1,2-oxazole N-oxide · Derivatives of 1,2-oxazole N-oxides · Aromaticity · DFT calculations

Introduction

Heterocyclic N-oxides constitute a valuable class of compounds [1, 2], used as protecting groups [3], auxiliary agents [4], oxidants [5], ligands in metal complexes [6], catalysts [7], intermediates in synthesis [1, 2] and as oxygen transfer agents in metabolic redox biological processes [7]. Their heteroaromatic congeners, particularly the 5- and 6-membered ones, have been taken as the subject of extensive research for many decades.

Electronic supplementary material The online version of this article (doi:10.1007/s11224-014-0459-6) contains supplementary material, which is available to authorized users.

P. Kozielewicz
School of Clinical and Experimental Medicine, University of Birmingham, Edgbaston, Birmingham B15 2TT, UK

D. Tzeli
Theoretical and Physical Chemistry Institute, National Hellenic Research Foundation, 48 Vassileos Constantinou Ave., 116 35 Athens, Greece

P. G. Tsoungas (✉)
Department of Biochemistry, Hellenic Pasteur Institute, 127 Vas. Sofias Ave., 11521 Athens, Greece
e-mail: pgt@pasteur.gr

M. Zloh
UCL School of Pharmacy, University College London, 29-39 Brunswick Square, London WC1 1AX, UK

M. Zloh
Department of Pharmacy, University of Hertfordshire, College Lane, Hatfield AL10 9AB, UK

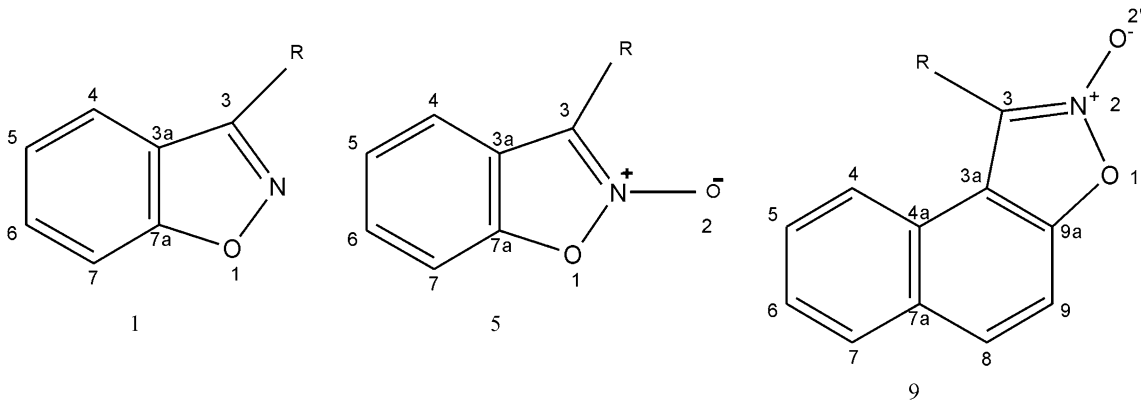

1 R = H
2 R = Me
3 R = Et
4 R = Ph

5 R = H
6 R = Me
7 R = Et
8 R = Ph

9 R = H
10 R = Me
11 R = Et
12 R = Ph

Fig. 1 1,2-Benzoxazole, N-oxide of benzo- and naphtho-fused 1,2-oxazole and their C-3 substituted compounds

The reactivity of N-oxides, dictated by the dual function of the N–O dipole, has drawn attention [1, 7]. In this context, the aromaticity concept [8–12] has been recruited, and a number of approaches, of varying applicability, have been developed to evaluate the aromaticity of carbocycles and heterocycles, using various indices [13–18]. Aromaticity is regarded as a statistically multidimensional concept [19–21], resting mainly on two orthogonal types, described as classical (referring to the energetic ASE and the structural I_A, HOMA indices) and magnetic (referring to the NICS index) [22], in accord with the principal component analysis [23]. These and many other indices have been applied to groups of molecules by many research groups over the years [24].

Reactivity parameters, such as chemical potential, electronegativity, hardness, electrophilicity, Fukui and Parr indices, numerically describe the corresponding chemical concepts [25]. In effect, they all refer to linear responses of electron density towards the variation of external potential and electron population. They are commonly used to predict, interpret or rationalize chemical bonding changes and reaction mechanisms.

1,2,5-Oxadiazole 2-oxides, commonly known as furoxans and their benzo-analogues [26–32], stand out as the most extensively studied structure of the 5-membered family. Other N-oxides of parent and benzo-fused heterocycles [33–41] have also been studied. Among them, the isoxazole ring occupies a prominent position, as a core structure, in many marketed drugs, such as penicillin antibiotics (cloxacillin, dicloxacillin, flucloxacillin), antipsychotic (risperidone, paliperidone) and COX 2 inhibitors (parecoxib) to name a few.

A closely related structure is that of the N-oxide of benzo- and naphtho-fused 1,2-oxazole (also called 1,2-benz(naphth)isoxazole) **5–8** and **9–12** (Fig. 1), respectively.

Some experimental data [42, 43] and early theoretical calculations [44] have shown a reactivity pattern, largely attributed to the electron donor–acceptor character of their N–O dipole.

Some reactivity features of **5** and **9**, discovered since then, resurged our interest in these structures. Quantum chemical calculations have been performed, herein, to probe the impact of the dipole on their geometry and aromaticity and ultimately lend support to the observed [42, 43] and predict their reactivity profile.

Methodology

All structures were fully geometry optimized via DFT calculations using the 6-31++G** basis sets [45], i.e. the B3LYP/6-311++G** methodology was used as implemented in ECCE/NWChem [46, 47]. The same software was used as a graphical interface for drawing and visualizing all structures. The B3LYP functional [48, 49] is a widely used functional and it is considered as a reliable one for the evaluation of geometries, energies and reactivity descriptors of 5-membered benzo-fused heterocycles [50]. Moreover, B3LYP credibility has been tested on the calculation of structure and reactivity profile of related systems such as β-nitroso-*o*-quinone methides [51], where B3LYP/6-31G**, B3LYP/6-311++G**, B3LYP/aug-cc-pVTZ, M06-2X/6-311+G**, M06-2X/aug-cc-pVTZ and MP2/6-311++G** calculations were performed. All methods resulted in similar data. Thus, we think that the B3LYP/6-311++G** methodology is a good one for the present study.

Geometry-based parameters, such as bond lengths, π-bond orders, total and relative energies, angles and dipole moments; reactivity descriptors, such as charge densities, chemical potential μ, chemical hardness η, frontier orbital energies, Fukui function $f(r)$ and local electro(nucleo)philicity Parr functions and aromaticity indices, such as Harmonic Oscillator Model of Aromaticity (HOMA) as well as bond uniformity (I_A) and average bond order/sum of bond order deviation (ABO/BOD), have been calculated to assess the effect of the N–O dipole on features of their structure, detect differences in their stability and reactivity and ultimately predict the reactivity profile of these heteroaromatic N-oxides.

Chemical potential μ [52, 53] and hardness η [21, 54] are expressed in terms of ionization potential I and electron affinity A as $\mu = -(I + A)/2$ and $\eta = (I - A)/2$ (or $\eta = (E_{LU} - E_{HO})/2$), respectively. The HO–LU gap (energy separation between highest occupied molecular orbital(HO) and lowest unoccupied molecular orbital(LU)) is known [55] to be related to stability, i.e. reactivity, and this relationship has been theoretically articulated as hardness η.

The Fukui function $f(r)$ [56, 57] represents the response of μ of a system to an external potential change, and it is expressed (in its condensed form) as $f_k^+ = [q_k\ (N + 1) - q(N)]$ or $f_k^- = [q_k(N) - q_k(N - 1)]$ or $f_k^\circ = [q_k(N + 1) - q_k(N - 1)]/2$ (where q_k is the electron population of an atom k and N the total number of electrons) towards nucleophiles, electrophiles or radicals, respectively.

Local electrophilicity ω_k [58, 59] and nucleophilicity N_K [58, 60] have been obtained through the Mulliken Population Atom Spin Density (ASD) analysis of the cation/anion radical formalism of the structures, using $\omega_k = \omega P_k^+$ and $N_k = NP_k^-$ equations.

Reformulated HOMA (rHOMA) index [54, 61–63] has been calculated by the delineated equation.

$$\mathrm{rHOMA} = 1 - \frac{\propto}{n}\sum_{i=1}^{n}\left(R_{opt} - R_i\right)^2,$$

where n is the number of bonds in the aromatic system. R_{opt} is the optimum bond length, and R_i is the real bond length of the i bond taken into consideration. This equation necessitates the use of the normalization constant α for each type of bond. The used values are $\alpha_{CC} = 257.7$ and $R_{opt} = 1.388$ for CC, $\alpha_{CN} = 93.52$ and $R_{opt} = 1.334$ for CN, $\alpha_{CO} = 157.38$ and $R_{opt} = 1.265$ for CO and $\alpha_{NO} = 57.21$ and $R_{opt} = 1.248$ for NO [62].

Bond order Uniformity index I_A [64–67] and ABO and its deviation (BOD) from ABO index [68–70] are statistical estimates of bond order variations. I_A index is based upon a statistical evaluation of the extent of variation of ring bond order provided by the expression:

$$I_A = 100F(1 - V/V_K),\ \text{where}\ V = \frac{100}{N}\sqrt{\frac{(N - \bar{N})^2}{n}}$$

$\bar{N}$ is the arithmetic mean of the n various ring bond orders, and N is the bond order. V_K is the value of V for the corresponding non-delocalised form of the ring, and F is the scaling factor [64–67].

Results and discussion

N-oxide structures such as **6–12** are built up by an oxidative *o*-cyclization of their precursor oximes of type **A** (*Z* or *E* isomers) (Scheme 1) [42, 43].

Pertinent to their formation is the loss of two σ electrons from **A** with subsequent dearomatization of the arene core to generate the transient *o*-quinone methides of type **B** (in either *Z* or *E* conformation) [51]. The geometry of the NO-carrying alkene arm of **B** (Scheme 1) resembles that of nitrosoalkenes [71–78] (Table 1) or the long-studied dinitrosoalkene, a transient intermediate in furoxan isomerization [26–31].

Indeed, the NO and C–C bonds of nitrosoalkenes compare well with those of the **B** *E* conformers. On the other hand, upon *o*-cyclization of the *Z* conformer of $\mathbf{B_1}$ or $\mathbf{B_2}$ to the N-oxide (Scheme 1), an elongation of the alkene C–C bond by ca. 0.09 Å and a shortening of C–N bond by ca. 0.11 Å, increasing its double bond character, are observed. Remarkably, the NO double bond remains unaltered. Substituents attached to the exocyclic alkene change the relative energy ordering of the of the *Z* and *E* conformers, probably, as a result of the relative spatial arrangement of *R* and NO groups (Table S1; Fig. 2S of the Supporting Information).

On the other hand, the incorporation of the N–O dipole in the arene-fused isoxazole structure triggers an energy drop in **5** and **9** (Table S2, Supporting Information). Indeed, the energy of **5** or **9** is much lower than that of their parent deoxygenated structures but closer to their corresponding **B** isomers [51].

Recent DFT calculations have unveiled [51] salient features of $\mathbf{B_1}$ and $\mathbf{B_2}$ and have provided a theoretical insight into the experimentally documented [42, 43] *o*- or *peri*-cyclization of $\mathbf{A_1}$ or $\mathbf{A_2}$. Accordingly, the NO group attached to the exocyclic alkene arm and the strained quinone structure trigger a 5-*exo-trig* *o*-cyclization[1] [51] and a concomitant aromatization to **6–8** or **9–12**. Very low energy barriers, in the range of 0.1–1.7 kcal mol^{-1}, elevated up to 4–7 kcal mol^{-1}, upon substitution at C-3, are

[1] C-3 unsubstituted **5** is not usually isolated; instead, it undergoes a *peri*(1,8)-(6-*endo-trig*)cyclization (see Ref. 43)

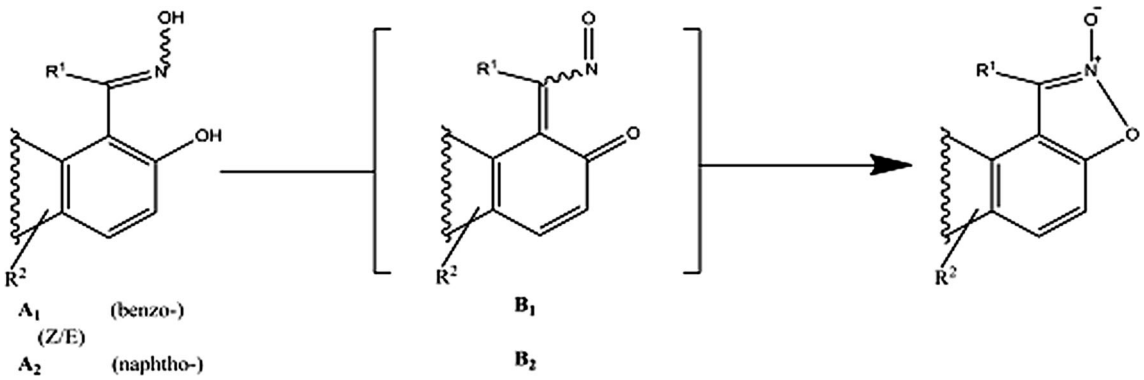

Scheme 1 Generation of N-oxide by oxidative cyclization of oxime $\mathbf{A_1}$ or $\mathbf{A_2}$ through *o*-quinone methide $\mathbf{B_1}$ or $\mathbf{B_2}$

Table 1 Bond lengths and bond orders of nitrosoethylene, N-oxides 5, 9 and *o*-quinone methides $\mathbf{B_1}$, $\mathbf{B_2}$ in *Z*/*E* conformations

	Nitrosoethylene[a]	**5**	**9**	$\mathbf{B_1}$ *Z*/*E*	$\mathbf{B_2}$ *Z*/*E*
C–C	1.335/1.333/1.361	1.426	1.423	1.426/1.361	1.422/1.363
	(2.008)	(1.635)	(1.649)	(1.635/1.961)	(1.648/1.951)
C–N	1.427/1.450/1.316	1.323	1.325	1.323/1.412	1.325/1.408
	(1.282)	(1.704)	(1.689)	(1.704/1.251)	(1.690/1.269)
N–O	1.215/1.211/1.192	1.215	1.217	1.215/1.222	1.212/1.224
	(1.877)	(1.924)	(1.910)	(1.924/1.885)	(1.911/1.874)

Values in parenthesis

[a] Transoid/cisoid/transition state, see Supporting Information, Fig. S1; bond orders of transoid

indicative of a virtually instantaneous cyclization of the in situ generated $\mathbf{B_1}$ or $\mathbf{B_2}$ (see Footnote 1).

Structure profile

Comparing the N-oxides **5–8** or **9–12** with their parent structures **1** or **2–4** (Fig. 1), the following features elucidate the impact of the N–O dipole on the geometry of the ring (Table S3, Supporting Information).

The ring N–O_1 bond of **5** or **9** is long (ca. 1.488 Å) and compares adequately with the most strained bonds in furoxans [26–31]. This bond is stretched by ca. 0.07Å in **5–8** or in their benzo-analogues **9–12** from that of their deoxygenated congeners (Table S3, Supporting Information). Of the C_3–N and $C_{7a(9a)}$–O_1 bonds, the former with a bond length of ca. 1.324 Å is longer by 0.02 Å from its deoxygenated counterpart, whereas the latter is unaffected. Interestingly, however, this bond, in the range 1.353–1.356 Å, implies some double bonding, conceivably the result of overlap of an O_1 lone pair with the ring π-orbitals. The C_3–C_{3a} bond of length ca. 1.425 Å and a bond order of ca. 1.640 also appear to 'feel' considerable π bonding.

On the contrary, the N–O_2 bond in both **5** and **9**, with a length of ca. 1.216 Å, falls in the range 1.202–1.258 Å, found in furoxans, [26–31] and it remains as short as in the NO_2 group. Its length, the bond order in the range of 1.910–1.924 and the extent of HO–LU localization (Fig. S3, Supporting Information) are indicative of its dipolar nature, though not as an isolated dipole but rather one with a substantial double bond character, a feature common to heteroaromatic N-oxides [1, 7]. Its double bond character is of the same magnitude with that of the NO group in **B** (Scheme 1). **5** or **9** can, thus, be regarded as the ring isomers of their open counterparts, *o*-quinone methides **B** (Table 1).

Worth noting, also, is that this double bond is shorter than that of the C_3–N bond. Clearly, the N–O dipole increases the π density in the hetero-ring through conjugation and brings about some π polarization. This accumulated π density compresses the bonds and induces ring strain [79] through its σ and π components, eventually causing some ring distortion.

This distortion, in **5–8** and **9–12**, is further enhanced by C-5 and C-6 substitution, exemplified in **13–16** and **17–20** (Fig. 2; Tables S4, S5, Supporting Information). These are the positions of most extended π conjugation with the respective ring O atom lone pair or the N–O dipole sites transmitted through the isoxazole ring π density.

The strong electron withdrawing NO_2 group appears to exert its impact over the whole bicyclic structure in **13**, **17** and **14**, **18**. Most notable are a C_{7a}–O bond length of 1.343 Å, implying some double bond character developing in that bond and an elongation (weakening) of the

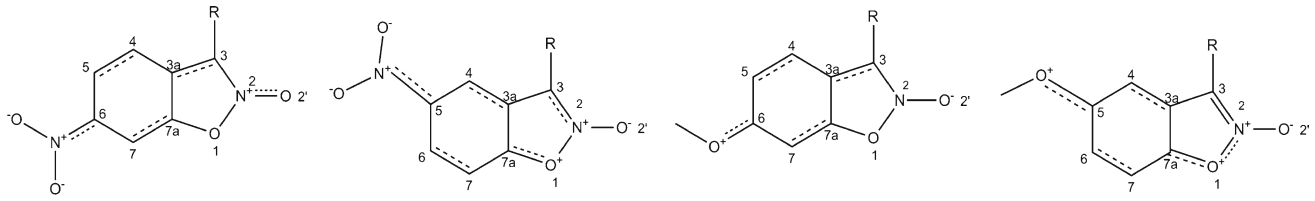

13 **14** **15** **16** R=H
17 **18** **19** **20** R=Me

Fig. 2 C-5 and C-6 substituted N-oxide of benzo-fused 1,2-oxazoles

Table 2 Calculated aromaticity indices for **1-4** and the N-oxides **5–20**

Compound number	I_A	HOMA	ABO/BOD
1	115.45	0.642	1.643/0.197
2	131.98	0.624	1.658/0.174
3	114.43	0.619	1.639/0.204
4	118.85	0.626	1.625/0.194
5	90.20	0.476	1.607/0.229
6	91.53	0.479	1.605/0.225
7	91.51	0.478	1.604/0.225
8	94.06	0.483	1.599/0.224
9	109.80	0.550	1.638/0.163
10	109.42	0.556	1.634/0.163
11	109.91	0.551	1.634/0.163
12	111.24	0.543	1.631/0.164
13	89.67	0.487	1.612/0.230
14	83.41	0.429	1.609/0.235
15	87.19	0.443	1.603/0.232
16	91.98	0.480	1.605/0.229
17	91.01	0.492	1.610/0.226
18	85.25	0.438	1.607/0.230
19	88.23	0.445	1.601/0.228
20	92.99	0.482	1.603/0.225

isoxazole ring N_2–O_1 bond with a bond length of 1.513 Å in **14** and **18.** In **13** and **17**, it is the π density of the benzene ring and a slight elongation of the C_3–N_2 bond that are affected. The strong electron releasing OMe group, on the other hand, appears to concentrate its influence on the ring O_1–N_2 and dipole N_2–O_2 bonds. A slight elongation in both is observed in **19**, while a shortening of the ring O_1–N_2 bond is found in **20**.

Bond length changes of ca. 0.007 and ca. 0.011 in **13** and **14**, respectively, as well as ca. 0.010 in **18** and ca. 0.006 in **17** are observed on either side of the *ipso* C-5 and C-6 substitution (Table S4, Supporting Information). The resonance effect of the NO_2 group in nitroarenes has been challenged [80–82], and it is its inductive ($-I$) effect that has been suggested [83] and confirmed [84] to account for its electron withdrawing power. The C_6–N bond length of 1.476 Å compares well with that of nitrobenzene [85], and it is not sensitive to the substitution site. Consistently, the bond alternation in benzene is only marginally affected by the NO_2 substituent at either position. This lends support to the earlier proposed weak π mesomerism of this group [84]. It also follows that there is no strong through-resonance interaction among NO_2 and N–O dipole. Significant changes of ca. 0.045 in **15** and ca. 0.013 in **19** but a relatively weaker one of ca. 0.009 in **20** are detected. These are considered as a result of the substituent sensitivity to bending and orientation and are most probably attributed to the Angular-Induced Bond Alternation (AGIBA) effect of this group, one of the best documented ones [86].

Reactivity profile

The indices I_A [34, 64–67], HOMA [54, 61–63] and ABO/BOD [68, 70] have been chosen as the most responsive to the changes imposed by the N–O dipole onto **1–4** as in bi(tri)cyclic structures **5–20** (Table 2). These indices detect deviations from a given reference state whether that be from bond order uniformity (I_A or ABO/BOD) or from an optimal bond length (HOMA, as in Kekulé benzene).

I_A values suggest that *N*-oxidation reduces the aromatic character of the bi(tri)cycle (Table 2). The reduction is more pronounced upon C-3 substitution in the range 20–31 %, even with the substituents of weak electronic effects. The largest drop (31 %) of the series is observed with **6.** On the other hand, an increase of 20–24 % in the aromatic character of the tricyclic structure is seen upon benzo-fusion, as in **9–12** (Table 2). Loss of aromaticity is also found upon 5- and 6-substitution, with substituents exerting strong electronic effects, as in **13–16** and **17–20**, consistent with earlier reports on the effects of substituents on aromaticity [24, 61–63]. However, while a drop, ranging from 0.5 to 7 % with respect to **5**, is seen in **13–16,** and a corresponding one of a similar range with respect to **6** is estimated for **17** and **18,** it is **19** and **20** that show a notable impact, a result of the OMe group AGIBA effect (see Tables S4 and S5) [86]. What is more interesting is that

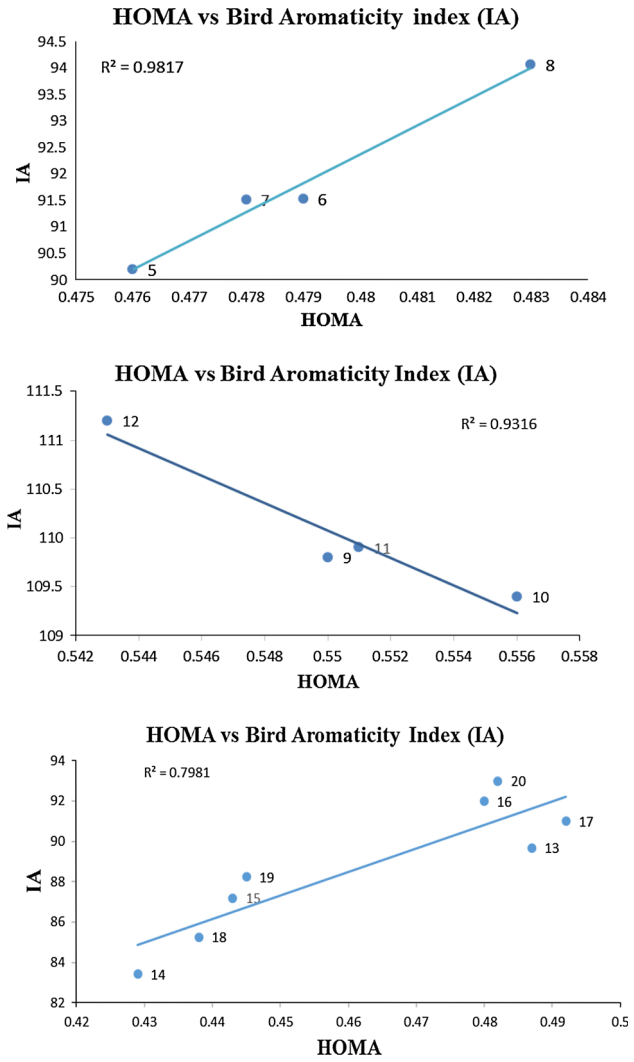

Fig. 3 HOMA versus I_A for the N-oxides **5–8**, **9–12** and **13–20**

marked changes occur when accompanied by C-3 substitution, particularly in **17** and **18** with a NO_2 group regardless of its position (Table 2).

HOMA values maintain a general consistency with the major features described with the I_A index, but they also record notable differences (Table 2). Thus, the N–O dipole does, indeed, cause a reduction of aromaticity by ca. 26 %, when comparing **5** to its deoxygenated **1.** On the other hand, an estimated 15 % increase of the HOMA value of **9**, when compared to **5**, demonstrates the stabilizing effect of benzo-annelation. C-3 substitution, as in **6–8**, shows a negligible increase from **5**, while no appreciable changes among them are detected. A change by ca. 1 % increments in **9–12** suggests a more pronounced impact of C-3 substitution.

ABO and BOD [68, 69] values demonstrate a notable destabilizing impact of the N–O dipole on the structure (Table 2). A ca. 2 % drop of ABO and a 15 % deviation (BOD) have been estimated upon incorporation of the N–O dipole in the hetero-ring. C-3 substitution does not perturb the π bond distribution. This is evident among both **5–8** and **9–12**. Benzo-fusion injects some stabilization by ca. 2 % (cf. **9** and **5**). C-5 and C-6 substitution seems to have no measurable effect on **13–16**, in contrast with **17–20** where the latter shows a distinct lower deviation, and **18** has the highest one. Similar trends are shown by hardness values [64, 67] (Table S6, Supporting Information), with **13** and **9** being the 'undisciplined' ones, both, however, unsubstituted at C-3.

Excellent correlations of HOMA versus I_A (Fig. 3) for the N-oxides **5–8** ($R^2 = 0.9817$) and **9–12** ($R^2 = 0.9316$) have been obtained. The reverse slope of the latter originates from their HOMA variations and is probably the result of the inherent diene character of their naphthalene core. Correlations of HOMA versus BOD as well as I_A versus ABO (Fig. S4 of the Supporting Information) indicate the obvious relation among these indices. Indeed, the lower the bond order deviation, the higher the delocalization and eventually the HOMA value. Similarly, the lower the bond order value, the higher will be the bond order uniformity I_A index. A moderate linear correlation ($R^2 = 0.7981$) has been estimated for the N-oxides **13–20** (Fig. 3). The strong electronic effects of their substituents disrupt the π delocalization, eventually increasing bond alternation and diene geometry, in particular. Poor correlation of these indices has been found in the parent isoxazoles **1–4** (Fig. S4 of the Supporting Information). This, probably, also reflects the greater bond localization (bond alternation) among the fused rings.

The N–O dipole increases the polarization of the π skeleton of the structure as shown by the dipole moments (Table S7, Supporting Information). *N*-oxidation raises the dipole moment of the bicycle by ca. 20 %. There is yet a further increase by C-3 substitution, as shown in **6–8**, in the range 26–29 %. Benzo-fusion does increase the polarization in **9–12**, only to a lesser extent 6–11 % (Table S7, Supporting Information).

Dipole moments of **13–16** and **17–20**, on the other hand, are derived from the combined strong electronic influence of the dipole and the nature and position of substitution (Table S7, Supporting Information). Values for 6-substituted **17** and **19** are higher by 28 and 14 %, respectively. These changes reflect the electron withdrawing effect of the former or the electron releasing effect of the latter in concert with the N–O dipole via the ring π density. Indeed, bond lengths of 1.382 Å for C_7–C_{7a}, 1.387 Å for C_4–C_5 and 1.330 Å for C_3–N_2 in **17** show C-6 to be the position of the most extended π conjugation. Remarkably, the N–O bond remains unaffected. Eventually, the corresponding aromaticity indices for these structures are the lowest of the series. A higher value recorded for **20** is a notable exception, apparently because its effect is mostly localized on the benzene ring.

Table 3 Calculated aromaticity indices I_A and HOMA of **1**, **5**, **6** and **9** compared with the literature values of other 1,2-oxazoles

Compound	I_A	HOMA
1,2,5-Oxadiazole[a]	53	0.677
1,2,3-Oxadiazole[b]		0.443
1,2,4-Oxadiazole[b,c]	48[c]	0.553
1,3,4-Oxadiazole[a]	62[c]	
Benzofuran[c]	106	
Benzofuroxan[d]	81	
Compound	**I_A**	**HOMA**
Isoxazole[a,e,f]	47[e] or 52[c]	0.527
Oxazole[b]		0.332
1,2-Benzisoxazole[e]	108, 115.4* (**1**)	0.642*
(2,1-Benzisoxazole)[a,e,g]	113	
N-oxide	90.2* (**5**)	0.476*
	91.5* (**6**)	0.479*
N-oxide	(**9**)	0.550*
	(**10**)	0.556*

* Our present work

[a] Ref. [67]

[b] Ref. [40]

[c] Ref. [67]

[d] Ref. [66]

[e] Ref. [64]

[f] Ref. [34]

[g] Ref. [91]

Aza-substitution (incorporation of N atoms) in a 6-membered ring is known [87] to trigger a small decrease of the aromatic character of the structure. A similar substitution in a 5-membered ring, however, is accompanied by a change of aromaticity, varying with the number and position of the N atoms in the structure [88, 89]. Qualitative observations suggest that more N atoms increase the aromaticity, while replacement of one or more by a more electronegative element, such as an O atom, causes its decrease. It may be argued that the π delocalization over the bi(tri)cyclic structure, a transition, in effect of π to π^* and n to π^* types, signifies a π electron transfer to antibonding orbitals from double bonds of the former type and from ring O atom p_z lone pair orbital of the latter type. However, the dual 'push–pull' character of the N–O functionality and the electronegativity of the ring O atom may hinder the n to π^* transfer. It has been suggested that O ring electronegativity contracts the p_z orbital and thus limits the n to π^* transfer, i.e. the lone pair overlaps with the ring π system [90].

Indeed, our calculations indicate higher aromaticity for 1,2-benzisoxazoles **1–4** compared with the reported estimates for parent isoxazole (Table 3). Their N-oxides suffer a decrease of aromaticity. The destabilizing effect of the N–O dipole is partly offset by the stabilizing benzo-fusion as exemplified in naphtho-fused analogues **9-12**.

A similar trend is also observed in the furoxan series (Table 3). Worth noting is that the influence of the *N* atoms on the aromaticity of these fused structures is not clear-cut, perhaps overpowered by that of the N–O dipole. From the preceding data, it would be safe to suggest that the N–O dipole enforces some diene geometry to the bi(tri)cyclic structures (i.e. induces some bond fixation), lowering the π delocalization and ultimately their aromatic character.

The highest occupied (HO) and the lowest unoccupied (LU) molecular orbitals occupy a large part of the structure (Fig. S3, Supporting Information). Both overlap extensively, mostly on the isoxazole ring. HO orbital is localized over this ring, particularly its N–O dipole, while its LU counterpart is almost spread over the entire structure. The previous orbital from HO (HO−1) is much less localized and is mainly spread over the carbocycle. The orbital after the LU orbital (LU + 1), on the other hand, shows a more extensive diffusion, encompassing the N–O dipole.

The energies of both HO and LU molecular orbitals (Table S8, Supporting Information) are sensitive to the N–O dipole. Thus, a ca. 10 % rise of the HO orbitals is accompanied by a drop of similar magnitude of the LU ones in **1–8** (Figs. S5–S7, Supporting Information). While the HO−1 orbital is virtually insensitive to the dipole, its LU+1 counterpart is drastically affected as shown by an estimated ca. 36 % energy drop. A ca. 5 % rise of the HO energy of **9** compared to **5** as well as a similar rise in **6–12**, accompanied by a 10–15 % drop of its corresponding LU are indicative of the effect of benzo-fusion. There is appreciable energy separation between HO and HO−1 or between LU and LU+1 orbitals. A marked separation among HO and LU (or among HO−1 and LU+1) is detected throughout the series of the N-oxides. C-3 substitution does not have any notable effect on the orbital energies of **6–8**. Their benzo- analogues **10–12** appear to be somewhat more vulnerable to C-3 substitution, showing a ca. 4 % rise of their HO, and a ca. 15 % decrease of their LU, **12** slightly falling off the overall trend with a tiny rise of its LU.

C-5 and C-6 substitution has a marked impact on HO (and HO−1) as well as LU (and LU+1) energies and their separation, when compared to **5** or **6,** as shown in **13–15** and **17–20** (Table S8; Fig. S7, Supporting Information). HO orbital is raised by a negligible 1 % in **13** and a notable 8 % in **14** and **15.** On the contrary, an energy drop of ca. 9 % in **18** and ca. 13 % in **17** is detected. Regioisomers **19** and **20** do not follow this trend showing a weak tendency to an energy rise by ca. 4 and 2 %, respectively. LU orbitals, on the other hand, are more drastically affected. An energy

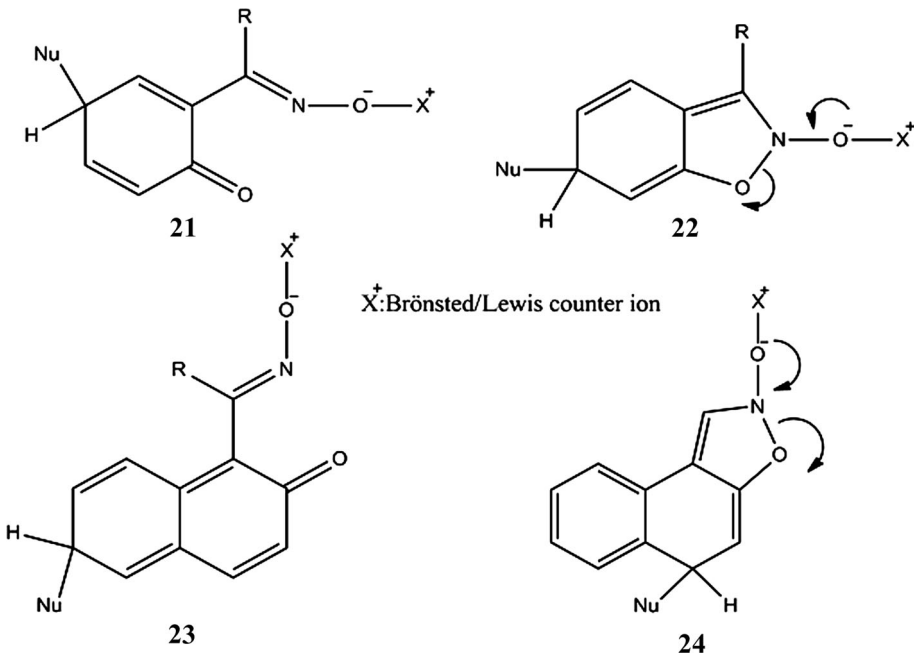

Fig. 4 Intermediates for the formation of the C-5 and C-6 substituted N-oxide of benzo-fused 1,2-oxazoles

drop of 50 % in **18** and 60 % in **17** is observed, whereas a rise of ca. 20 % is shown for **19** isomer and a very moderate 5 % rise for **20** one. A similar trend is followed by the HO−1 orbitals with energy drops of ca. 7 % in **13** and **14** and a ca. 11–12 % drop in **17** and **18. 15**, **19** and **20**, consistently off-course, appear either insensitive or with a propensity to an energy rise. LU+1 orbitals are more sensitive, exhibiting energy drops of ca. 80 and 70 % in **17** and **18,** respectively, with **19** and **20** towards an energy rise.

Clearly, quite marked energy changes are recorded for the HO and LU (or HO−1 and LU+1) orbitals. Thus, a HO-LU gap of ca. 0.1 Hartrees (or ca. 63 kcal mol^{-1}) and a HO−1 − LU+1 gap of ca. 0.24 Hartrees (or ca.150 kcal mol^{-1}) [92, 93], for the N-oxides **5–20**, qualifies them as structures of notable aromaticity.

These observations lend support to the dual 'push–pull' nature of the dipole. It is known [92–95] that HO orbital is related to ionization potential, and the LU one to electron affinity, hence their susceptibility to electrophiles or nucleophiles, respectively. It is, therefore, anticipated that electrophiles can attack the carbocycle at C-6 in **5**, **6–8** or C-8 in **9–12**, whereas nucleophiles can attack at C-6 and C-7 in **5**, **6–8** or C-6 and C-8 in **9–12**, through activation, in both cases, by the N–O dipole. These predictions are confirmed by the Mulliken charges (Table S9, Supporting Information), Fukui indices (Table S10, Supporting Information) and Parr (ω_k) and Nucleophilicity (N_k) indices (Table S11, Supporting Information).

Interestingly, C-6, C-7, C-8 or C-9 emerge as primary sites for electrophilic and nucleophilic attack, respectively. Calculations also point to C-4 and C-5 as alternative sites of attack, only to a much lesser extent. The data are in line with experimental results [42] for attack by electrophiles. However, it has been shown [42] that a nucleophilic attack is not as predictable. Thus, site selectivity appears to depend on or even be dictated by the weakness of the ring N–O bond (Fig. 4; Table 3S, Supporting Information). This bond does not survive a nucleophilic attack and suffers a reaction medium-driven rupture. Fukui values indicate C-4 and C-6 in **5**, **6–8** and C-8 or C-9 in **9–12** as main sites for the attacking nucleophile. Parr indices, on the other hand, suggest C-6 and C-8 as major sites for attack for **5** and **9**, respectively. Experimental findings confirm C-5 and C-6 as the substitution products [42].

Cardinal to both types of site selectivity is the 'push–pull and double bond character of the N–O dipole against the reaction medium. Calculated predictions (referring to an isolated molecule), in line or partly at variance with experimental data, point to the double bond nature of the dipole as probably being the major determinant of the outcomes. To that end, a rationale for both types of reactions is laid out.

In the usually strongly acidic environment of an electrophilic attack, the susceptibility of the carbocycle towards it, i.e. its π density, seems to be virtually undisrupted. This is so, because any interference expected from protonation of or a coordination with the N–O dipole, in the reaction medium, hampering the reaction, seems to be rather weak due to the limited availability of the charge on the O atom (N–O dipole with a π bond order of ca. 1.910). The 'push' component of the dipole can, thus, activate the particular sites towards the attacking electrophile. On the contrary, any bonding interaction of the N–O dipole with

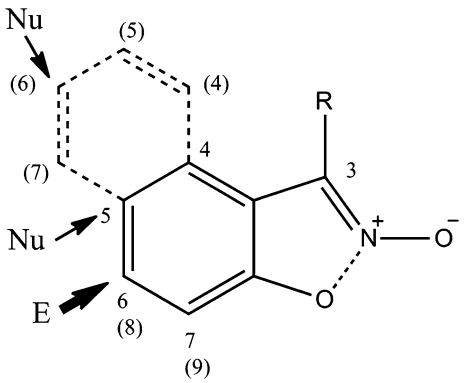

Fig. 5 Reactivity pattern of the N-oxide benzo-and naphtho-fused 1,2-oxazoles (*E* electrophile, *Nu* nucleophile)

the counterion of the attacking nucleophile; however, weak it may be, compresses the weak ring N–O bond, causing its rupture, presumably before the 'pull' component of the dipole (through the charged N atom) takes to effect. Thus, predicted site selectivity could be depicted by intermediates of type **22** and **24** (Fig. 4), whereas experimental evidence would favour intermediates of type **21** and **23** (Fig. 4).

Relative energies favour the quinonoid arrangement of **21** and **23** as more stable structures (Fig. 4). It is, therefore, reasonable to suggest that it is the ring opening the source of any discordance between the calculated and actually observed site selectivity in nucleophilic substitution.

On the basis of the outlined arguments, the reactivity pattern of the N-oxide structure can, thus, be safely deduced as shown (Fig. 5).

Conclusion

N–O dipole, benzo-fusion (some bond localization) and C-3 substitution are the main determinants of the geometry distortion and aromatic character of **5–20,** as measured by I_A, HOMA and ABO/BOD indices. It is the 1,2-oxazole (isoxazole) ring that suffers most of the distortion, while the fused carbocycle (benzene or naphthalene) is much less affected. Calculated data adorn the N-oxides with a signature of notable aromatic character. The predicted reactivity pattern indicates susceptibility at C-6, C-7 and C-8 towards electrophiles or nucleophiles, respectively. Calculations for electrophilic substitution appear to be largely in good agreement with experimental outcomes. A discrepancy, however, between calculated (at C-6 or C-8) and observed (at C-5 or C-6) site selectivity has been realized in nucleophilic substitution and has been attributed to the propensity of the ring N–O bond to rupture upon a nucleophilic attack.

Site selectivity is directed by the dual ('push–pull') character of and the double bonding in the N–O dipole. The latter feature, in particular, appears to be the major determinant that can account for the calculated outcomes and their relation to the experimental results.

References

1. Alvarez-Builla J, Vaquero J, Barluenga J (2011) Modern heterocyclic chemistry, chapt. 13, vol 1. Wiley, Weinheim
2. Sivasubramanian G, Parameswaran VR (2007) J Heterocycl Chem 44:1223–1230 (references cited therein)
3. MacCoss M, Ryu EK, White RS, Last RL (1980) J Org Chem 45:788–794
4. Iwamatsu K, Shudo K, Okamoto T (1983) Heterocycles 20:5–8
5. Albini A (1993) Synthesis 1993:263–277
6. O'Connor CJ, Sinn E, Carlin RL (1977) Inorg Chem 16:3314–3320
7. Albini A, Pietra S (1991) Heterocyclic N-oxides. CRC Press, Boca Raton
8. Alkorta I, Elguero J (2009) In: Gupta RR, Krygowski TM, Cyrański MK (eds) Topics in Heterocyclic Chemistry, vol 19. Springer, New York
9. Stanger A (2009) Chem Commun 15:1939–1947
10. Fowler PW, Lillington M, Olson LP (2007) Pure Appl Chem 79:969–980
11. Krygowski TM, Stepień BT (2005) Chem Rev 105:3482–3512
12. Irina V (2012) Omelchenko Oleg V. Shishkin •Leonid Gorb • Frances C. Hill • Jerzy Leszczynski. Struct Chem 23:1585–1597
13. Giambiagi M, Segrede Giambiagi M, dos Santos Silva CD, de Figueiredo AP (2000) Phys Chem Chem Phys 2:3381–3392
14. Kotelevskii SI, Prezhdo OV (2001) Tetrahedron 57:5715–5729
15. Rassat A (2004) Phys Chem Chem Phys 2:232–237
16. Aihara JI (2006) J Am Chem Soc 128:2873–2879
17. Matito E, Salvador P, Duran M, Solá M (2006) J Phys Chem A 110:5108–5113
18. Zubatyuk RI, Shishkin OV, Gorb L, Leszczynski J (2009) J Phys Chem A 113:2943–2952
19. Noorizadeh S, Shakerzadeh ES (2010) Phys Chem Chem Phys 12:4742–4749
20. Bird CW (1998) Tetrahedron 54:14919–14924
21. Alonso M, Herradón B (2010) J Comput Chem 31:917–928
22. Omelchenko IV, Shishkin OV, Gorb L, Leszczynski J, Fiase S, Bultinck P (2011) Phys Chem Chem Phys 13:20536–20548
23. Katritzky AR, Karelson M, Sild S, Krygowski TM, Jug K (1998) J Org Chem 63:5228–5231
24. OmelchenkoIV, Shishkin OV, Gorb L, Hill FC, Leszczynski J (2013) Struct Chem 24:725–733 (references therein)
25. Chandra AK, Nguyen MT (2002) Int J Mol Sci 3:310–323
26. Yu ZX, Caramella P, Houk KN (2003) J Am Chem Soc 125:15420–15425 (references cited therein)
27. Rauhut G (2001) J Org Chem 66:5444–5448
28. Eckert F, Rauhut G, Katritzky AG, Steel AR (1999) J Am Chem Soc 121:6700–6711
29. Klenke B, Friedrichsen W (1998) J Mol Struct (Theochem) 451:263–267
30. Eckert F, Rauhut G (1998) J Am Chem Soc 120:13478–13484
31. Chiari G, Viterbo D (1982) Acta Cryst B38:323–325
32. Kwiatkowski JS, Leszczynski J, Teca I (1997) J Mol Struct 436–437:451–480
33. Boiani M, González M (2005) Mini Rev Med Chem 5:409–424
34. Bird C (1987) Tetrahedron 43:4725–4730

35. Domene C, Jenneskens LW, Fowler PW (2005) Tetrahedron Lett 46:4077–4080 (references cited therein)
36. Alvarez-Builla J, Vaquero JJ, Barluenga J (2011) Modern heterocyclic chemistry, Chapt. 12, vol 1. Wiley, Weinheim
37. Lakhdar S, Goumont R, Boubaker T, Mokhtari M, Terrier F (2006) Org Biomol Chem 4:1910–1925
38. Lee GT, Jiang X, Vedananda TR, Prasad K, Repič O (2004) Adv Synth Catal 346:1461–1464
39. Ravi P, Gore GM, Tewari SP, Sikder AK (2012) Mol Simul 38:218–226
40. Schmidt A, Dreger A (2011) Curr Org Chem 15:1423–1463
41. Alkorta I, Elguero J, Liebman JF (2006) Struct Chem 17:439–444
42. Boulton AJ, Tsoungas PG, Tsiamis C (1987) J Chem Soc Perkin Trans 1:695–697
43. Supsana P, Tsoungas PG, Aubry A, Skoulika S, Varvounis G (2001) Tetrahedron 57:3445–3453
44. Tsoungas PG, Tsiamis C, Michael C, Sigalas M (1987) Tetrahedron 43:785–790
45. Curtiss LA, McGrath MP, Blandeau JP, Davis NE, Binning RC Jr, Radom L (1995) J Chem Phys 103:6104–6113
46. Valiev M, Bylaska EJ, Govind N, Kowalski K, Straatsma TP, Van Dam HJJ, Wang D, Nieplocha J, Apra E, Windus HJJ, de Jong W (2010) Comput Phys Commun 181:1477–1489
47. Sloot PA, Abramson D, Bogdanov A, Gorbachev Y, Dongarra J, Zomaya A, Black G, Schuchardt K, Gracio D, Palmer B (2003) Computational science ICCS. Springer, Berlin Heidelberg, pp 122–131
48. Becke D (1993) J Chem Phys 98:1372–1377
49. Lee C, Yang W, Parr RG (1988) Phys Rev B 37:785–789
50. Jursic BS (1998) J Mol Struct (THEOCHEM) 427:165–170 (references cited therein)
51. Kocielewicz P, Tsoungas PG, Tzeli D, Petsalakis ID, Zloh M Struct Chem. doi:10.1007/s11224-014-0454-y
52. Domingo LR, Pereza P, Contreras R (2004) Tetrahedron 60:6585–6591
53. Parthasarathi R, Padmanabhan J, Elango M, Subramanian V, Chattaraj PK (2004) Chem Phys Lett 394:225–230
54. De Proft F, Geerlings P (2001) Chem Rev 101:1451–1464
55. Pearson RG (1993) Acc Chem Res 26:250–255
56. Gonzalez-Suarez M, Aizman A, Soto-Delgado J, Contreras R (2012) J Org Chem 77:90–95
57. Fuentealba P, David J, Guerra D (2010) J Mol Struct 943:127–137
58. Domingo LR (2013) RSC Adv 3:1486–1494
59. Chattaraj PK, Giri S, Duley S (2011) Chem Rev 111:PR43–PR75
60. Pratihar S, Roy S (2010) J Org Chem 75:4957–4963
61. Raczyńska ED, Hallman M, Kolczyńska K, Stępniewski TM (2010) Symmetry 2:1485–1509
62. Frizzo-Marcos CP, Martins AP (2012) Struct Chem 23:375–380
63. Krygowski TM, Ejsmont K, Stepień BT, Cyrański MK, Poater J, Solá M (2004) J Org Chem 69:6634–6640
64. Bird CW (1997) Tetrahedron 53:3319–3324
65. Bird CW (1996) Tetrahedron 52:9945–9952
66. Bird CW (1993) Tetrahedron 49:8441–8448
67. Bird CW (1992) Tetrahedron 48:335–340 and 1675–1677
68. Matito E, Salvador P, Duran M, Solà M (2006) J Phys Chem 110:5108–5113
69. Jursic BS (1997) Tetrahedron 53:13285–13294
70. Jursik BS (1997) In: Párkányi C (ed) Theoretical organic chemistry, vol 15. Elsevier, New York, p 530
71. Bodnar BS, Miller MJ (2011) Angew Chem Int Ed 50:5630–5647
72. Yang B, Zöllner T, Gerbhardt P, Möllmann U, Miller MJ (2010) Org Biomol Chem 8:691–697
73. Li P, Majireck MM, Witek JA, Weinreb SM (2010) Tetrahedron Lett 51:2032–2035
74. Tsoungas PG (2002) Heterocycles 57:1149–1178
75. Tsoungas PG (2002) Heterocycles 57:915–953
76. Lyapkalo IM, Ioffe SL (1998) Russ Chem Rev 67:467–484
77. Sarasola C, Cossío FP, Ugalde JM (1990) Can J Chem 68:762–769
78. Bean GP (1998) J Phys Chem 63:2497–2506
79. Stanger A, Ben-Mergui N, Perl S (2003) Eur J Org Chem 2003:2709–2712
80. Lipkowitz KB (1982) J Am Chem Soc 104:2647–2648
81. Hiberty PC, Ohanessian G (1984) J Am Chem Soc 106:6963–6968
82. Topsom RD (1987) Prog Phys Org Chem 16:85–125
83. Smith MB, March J (2001) Advanced organic chemistry: reactions, mechanisms and structure, 5th edn. Wiley Interscience, New York
84. Boese R, Bläser D, Nussbaumer M, Krygowski TM (1992) Struct Chem 3:363–368
85. Irle S, Krygowski TM, Niu JE, Schwarz WHE (1995) J Org Chem 60:6744–6755
86. Krygowski TM, Cyrański MK (2003) Synlett 7:922–936
87. Katritzky AR, Jug K, Oniciu DC (2001) Chem Rev 101:1421–1449
88. Cyrański MK, Krygowski TM, Katritzky AR, von Raguer Schleyer P (2002) J Org Chem 67:1333–1338
89. Nyulászi L, Várnai P, Veszpremi T (1995) J Mol Struct (Theochem) 358:55–61
90. Cordell FR, Boggs JE (1981) J Mol Struct (THEOCHEM) 85:163–178
91. Matos MAR, Miranda MS, Morias VMF, Liebman JL (2004) Eur J Org Chem 2204:3340–3345
92. Vektariene A, Vektaris G, Svoboda J (2009) ARKIVOC vii:311–329
93. Bean GP (1998) Tetrahedron 54:15445–15456
94. Domingo LR, Chamorro E, Pérez P (2008) J Org Chem 73:4615–4624
95. Domingo LR, Pérez P (2011) Org Biomol Chem 9:7168–7175